Microstructural Science Volume 27

Understanding Processing, Structure, Property, and Behavior Correlations

31 October–3 November 1999

CONFERENCE PROCEEDINGS

William N. Weins

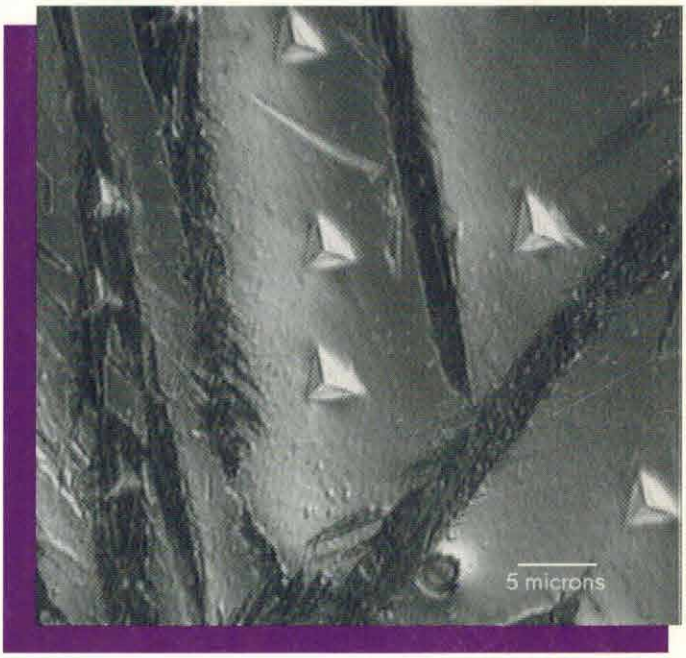

IMS
International Metallographic Society

ASM INTERNATIONAL®
The Materials Information Society

Microstructural Science Volume 27, 31 October–3 November 1999, Cincinnati, Ohio, ASM International, 2000

Thixomet Image Analyzer for Characterization of 2D and 3D Materials Structure

A.A. Kazakov, N.H. Luong, E.I. Kazakova, E.M. Zorina
St. Petersburg State Technical University
St. Petersburg, Russia

Abstract

Capabilities of the Thixomet Image Analyzer for two- and three-dimensional material microstructural characterization are demonstrated with examples of aluminum-based semi-solid materials (Thixomet software) and nickel-based superalloys (Thixomet SAQE software). Practical use of the Thixomet family of products for controlling material properties by controlling their microstructure is demonstrated.

Introduction

One of the most common uses of Image Analysis Systems (such as the Quantimet, Omnimet, Clemex, Leco and others) is a quality estimation of a material's structure. However, it is not uncommon that the capabilities of these image analyzers are insufficient for solving certain specific technological problems, especially those involving new materials.

This paper describes the Thixomet Image Analyzer, which has the ability to conduct quality control studies of metallic material structures including the estimation of its three-dimensional parameters. The Thixomet system also provides the most commonly used metallographic evaluation methods, implemented in the above-mentioned commercial image analysis systems.

The lack of domestic industrial image analyzers in Russia is another reason which induced the authors, being experts in the field of steel making processing, to develop an instrument for quality estimation of microstructure. The absence of Russian-designed image analyzers does not mean that there is a lack of theoretical studies in quantitative metallography in Russia. The classic publications of the late Ervin E. Underwood, such as his book, Quantitative Stereology [1], were stimulated by his (and several colleagues) efforts to translate the 1958, second edition, of the landmark text of Sarkis A. Saltykov [2] who developed a scientific foundation for stereological methods in materials science in Russia. Saltykov's work has become the foundation for the majority of the quantitative materials science research studies throughout the world.

The recent progress in computer hardware design and production, appearance of less expensive powerful devices, like high-resolution CCD cameras and frame grabbers, and the advanced development systems have reached the level sufficient for comprehensive digital image processing. Thus, the theoretical foundations of quantitative metallography and image processing [1-4], and the technical progress in computer technologies and digital television have made possible the creation of the Thixomet Image Analysis System.

Thixomet software is a family of products, which includes image analysis software for the quality estimation of the structure of various materials [5-8] and provides solutions for many specific technological problems.

Thixomet Image Analyzer capabilities will be demonstrated using examples of nickel-based superalloys and aluminum-based Semi-Solid Materials (SSM) taking into account the theme of this conference: "Understanding Processing - Structure - Property - Behavior Correlations".

Metallurgical Quality Characterization of Nickel-based Superalloys

Special features of the technology. It is well known that the technology of production of finished parts from superalloys (for example, turbine blades) includes several stages. First, the billets are produced from the original charge materials in large vacuum induction furnaces. Then the slugs are machined from the billets and used in small induction furnaces for the production of finished parts by investment casting. As a result, a large quantity of scrap results from this method of casting and as a consequence the recycling problem appears. However, the scrap fraction in the VIM charge for billet production should not be above about 30%, as a rule. It is possible to increase the fraction of the scrap in the charge if it has been previously remelted using active refining melt technology. Therefore, not only the chemistry of the billet, obtained by the refining of the scrap, must be checked, but

also the billet's metallurgical quality must be examined before it is used for turbine blades.

Principle of estimation method. The well-known quality estimation method of Willan Metals Company has been taken as a basis. According to this procedure, a specimen is examined metallographically at 200× to evaluate the impurity of the metal by the determination of the impurity rate. The specimen is machined from the bottom part of the cylindrical billet. The surface area to be examined is equivalent to the area of a circle with the diameter of 20 millimeters. The total area of the cross section is observed sequentially, field by field.

The types of superalloy impurities are sorted by their size at 200×:

Oxide film (OF) is characterized by its size:

- a "large" film has a size equal to the diameter of the field of view;
- a "middle" film has a size equal to one-half of the diameter of the field of view; and,
- a "small" film has a size equal to one-fourth of the diameter of the field of view.

Slag globules (SG) and nitride clusters (NC) are characterized by size:

- a "large" one occupies one-tenth of the field of view area;
- a "middle" one occupies one-fiftieth of the field of view area; and,
- a "small" one occupies one-hundredth of the field of view area.

The total rate is calculated from the following equation with regard to the contribution of each impurity type revealed on n-observed fields of view:

$$R_{\Sigma} = \sum_{i=1}^{n} \sum_{j=1}^{3} \sum_{k=1}^{3} \left(R_{j,k} \cdot N_{j,k}^{i} \right), \qquad (1)$$

where $R_{j,k}$ is the rate coefficient for defect j of k-dimensional group and $N_{j,k}^{i}$ is the number of defects j of k-dimensional group on the field of view i.

The following rates are defined by the expert estimation approach for each impurity type:

- for oxide films and slag globules $R_{j,k}$ is equal to 1, 0.5 and 0.25 for large, middle and small defects, respectively;
- for nitride clusters $R_{j,k}$ is equal to 10, 5 and 2 for large, middle and small defects, respectively.

It should be noted that the rate for nitride clusters is 10 times higher than for slag globules in the same dimensional group. It depends upon the fact that nitrides and their clusters are more difficult to remove from superalloy melts than slag globules, which are easily assimilated by the refractory lining of the crucible during remelting or by the ceramic surface of the filter during pouring.

The Thixomet SAQE software has been developed for automation of the measurements required for this approach. Unique methods of quantitative metallography have been successfully applied in Thixomet SAQE that result in increased accuracy in determining a defect's dimensions. The defect's size measurements provided in Thixomet SAQE are more precise than visual estimation by operator. Therefore, it was possible to use an improved method of impurity estimation by a monotonic function of the defect rate versus its dimension instead of the three-stepped function of the Willan Metals' procedure.

The strategy for the Thixomet SAQE procedure can be summarized as follows. The images with metallurgical impurities (oxide films, slag globules and nitride clusters) are transmitted through the CCD camera and frame grabber to the image analyzer monitor. The sharpness adjustment has to be carried out so that the carbides and nitride clusters have uniformly colored surfaces. Then, the image is captured and processed (Fig.1).

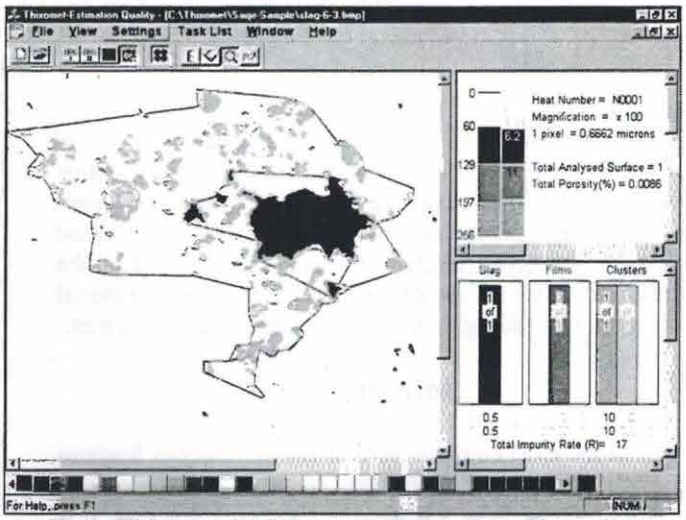

Fig.1. Thixomet SAQE screen. Estimation of impurity rate

Defect identification is performed according to the complex criteria that includes information on the grayscale level of the objects (1), their morphology (2) and the nature of mutual arrangement (3). The grayscale level for each defect is pre-adjusted. For this purpose, there are threshold levels on the Thixomet control panel. Carbide and nitride inclusions have close grayscale levels, so they cannot be separated using this criterion. To separate them, the character of their mutual arrangement is estimated. The carbides, which are uniformly distributed across the cross section, are automatically removed from the analysis.

The image processing results are presented as a bar chart, which depicts the quantity for each type of defects. These bar charts are displayed in one of the operating windows of the Thixomet SAQE. The total impurity rate of the investigated sample, as well as specific rates for each type, is shown here as an accumulated sum (Fig.1).

Film elongation is calculated as for a continuous linear feature; in this case the breaks in films are connected. The area occupied by slag globules and nitride clusters is estimated by the area of the figure, which is formed by the external boundary of the defect conglomeration. When evaluating the area, occupied by nitride clusters, the user is able to modify

the clustering rate either by joining the inclusions to the cluster or by integration/separation of neighbor clusters (Fig.2).

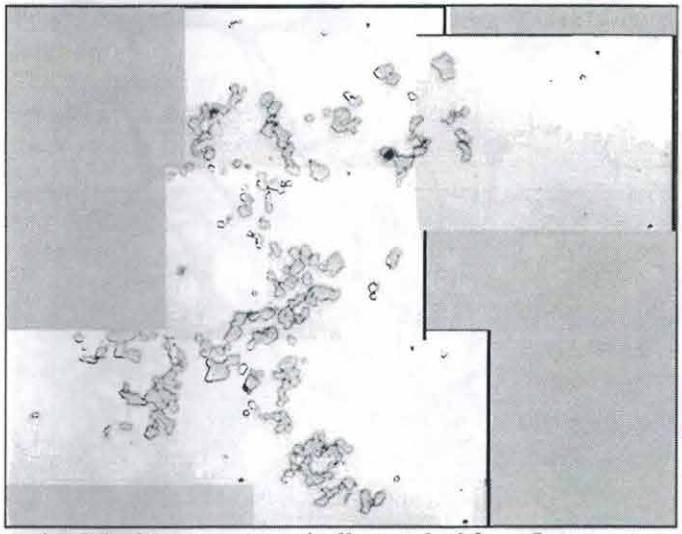

a) original image automatically matched from 5 segments

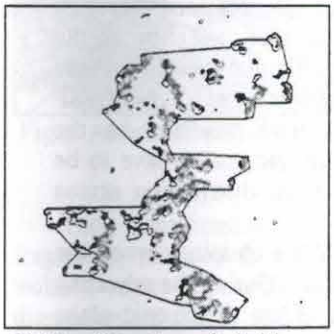

b) identification of nitrides as one big cluster

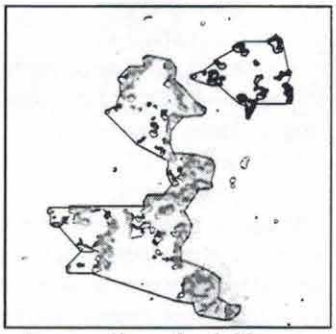

c) separation of neighbor clusters

Fig.2. Nitride cluster identification

There could be cases when the metallurgical defect does not fit a translating monitor. Decreasing the microscope magnification is undesirable because it may lead to loss of resolution necessary for correct identification of the defects and precise measurement of their sizes. To overcome this problem, a special procedure was developed in Thixomet for the reconstruction of the full defect image by sequential capture and perfect matching of its segments. A microstructural montage of segments into a full image of the defect is carried out automatically according to a specially developed algorithm. Creation of the full image of the defect can be observed at the Thixomet main window (Fig.2a).

Another unique procedure of Thixomet SAQE corrects some of the defects in images. This procedure removes the scratches and corrects the nonuniform illumination present in optical systems. It is automatically performed in real-time mode before each measurement (Fig. 3).

The decision to use the charge billet in the production of turbine blades is based on metallurgical quality estimation results. Billets with an impurity rate more than a limiting value are remelted using the refining technology. The limiting value of the impurity rate for the charge billet is established by standard technical documentation.

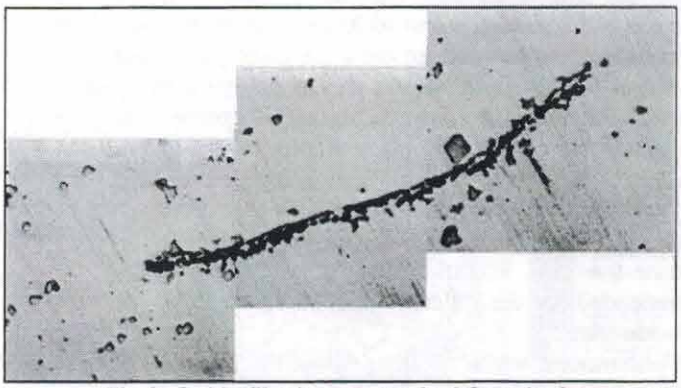

Fig.3. Oxide film image matched from its 3 segments

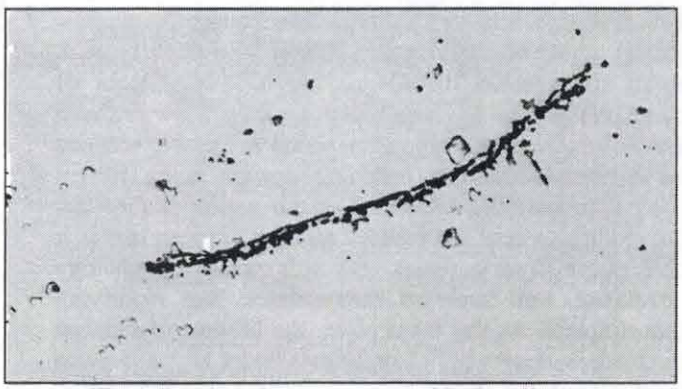

Fig.4. Previous image processed by leveling procedure

So, the main capabilities of Thixomet SAQE are the following:

1. precise matching of the images with each other, obtained by the successive import of adjacent fields of view, permits:
   - creation of a panorama image;
   - high resolution capacity while investigating the large area of the object;
   - new possibility for quantitative analysis of the material structure without excluding marginal objects;
2. leveling of nonuniform illumination of the reflection light microscope image and removal of scratches from the surface of cross-section;
3. identification of structure objects using one or several criteria, e.g., grayscale level, morphology factors, and the pattern of the mutual arrangement of the objects; and,
4. estimation of total and specific impurity rates.

The additional capabilities of Thixomet SAQE include the estimation of porosity content in blade test sections and manual measurements operations of the features.

Improvement of the technology by controlling microstructure. Since 1998, the Thixomet Image Analyzer and the SAQE program have been used at the St.-Petersburg Turbine Blades Plant (Russia) for metallurgical quality estimation of all billets used in the production of turbine blades. This experience of the Thixomet SAQE application under the plant conditions has demonstrated it's high

performance. Rejects have decreased because of elimination of charge billets with insufficient metallurgical quality from production. The analysis of quality estimation results has made it possible to obtain new technological information. This information could be used for the analysis of production state as well as for the development of technology improvement methods. For example, the availability of specific impurity rates allows the correct refining technology for a given batch of billets to be found. So, high-temperature treatment of the melt should be recommended for billets with a high rate of nitride cluster impurities to dissolve the nitrides and to denitrate the melt. Filtration refining of the melt should be recommended for the billets with high rate of slag globules and oxide films.

Furthermore, while speaking about the nitrogen refining of the melt, it should be mentioned that currently the consumers of superalloys impose limitations on nitrogen contents in charge billet to ≤ 0.002 wt. %. But this limitation is not based upon sound reasons. There are carbides with extremely unfavorable shape (i.e., highly elongated or as "Chinese hieroglyphs") within billets with such low nitrogen contents. Carbides of this type are inherent in massive sections of the blades and induce polishing cracks during further mechanical processing. As shown in our earlier studies [8], precise modification of the melt by gaseous nitrogen makes it possible to transform carbides with unfavorable morphology into equiaxial, well-dispersed carbonitrides, thus modifying the cast structure. As this takes place, the lifetime of finished turbine blade increases by 1.5 or 2 times under normal service conditions. Thus, the charge billet has to be controlled both in the metallurgical quality and the morphology of the carbides. As for the billets with unfavorable morphology of the carbides, precise nitrogen modification of the melt before blade production is recommended.

Characterization of Semi-Solid Materials Structure

Advantages of semi-solid forming (SSF) technology in comparison with conventional casting methods, as well as its considerable progress, are well known [9]. But there are still many problems hindering full application of this technology. In order to solve these problems successfully, it is necessary to develop a special tool for objective quality estimation of semi-solid materials (SSM) structure at all stages of their production.

Al-Si alloys, such as A356/357, are widely applied in SSF technology. The structure of these alloys consists of alpha solid-solution aluminum grains surrounded by the alpha-Si eutectic (Fig.5). The SSF technology is based on the peculiarities of rheological behavior of semi-solid materials. In turn, the rheological characteristics depend on alpha solid-solution morphology. Therefore, the characterization and control of alpha solid-solution morphology at each stage of SSF technology are of prime importance for a successful realization of this technology.

Semi-solid materials structure. The SSF technology will be discussed in respect to the requirements that can be imposed on image analysis in quality estimations of SSM structures.

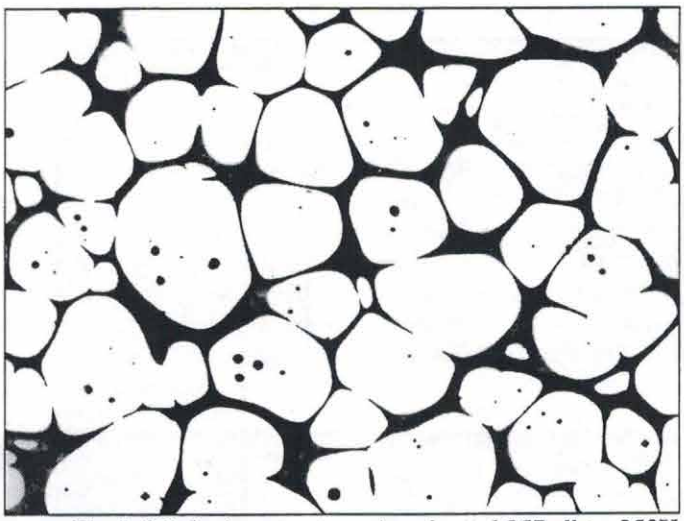

Fig.5. SSM microstructure. As reheated 357 alloy, 250X

Rheocasting is the first stage of SSF technology, when a thixotropic (nondendritic) structure is obtained through magneto-hydrodynamic stirring (MHD) of the alloy at the solidification front. It is only rheocasting that lays the ground for the further evolution of the structure at other stages of SSF technology. There must not be typical dendrites in the structure of the billet. The fine thixotropic grains have to be minimally agglomerated, and the silicon distribution across the billet diameter has to be uniform.

Reheating is the next stage of SSF technology when the slugs are heated in the induction furnace. During the reheating cycle, the important globularization of the thixotropic alpha solid-solution grains occurs. Associated negative processes, such as structure coarsening, formation of occluded eutectic and further structure skeletonization, which started during rheocasting, also take place here. The chosen reheating temperature-time parameters must promote globularization of the thixotropic grains while limiting, as much as possible, the detrimental processes.

Forming is the final stage of SSF technology, which is entirely dependent on the previous stages. In the casting machine, the ram injects the slug into the die cavity and applies the pressure to produce the thixotropic castings.

The above-enumerated special features of SSF technology produce the microstructural features, which establish the requirements placed upon the image analyzer for the estimation of the quality of the SSM structure.

The principal capabilities of Thixomet for characterization of SSM structure. Thixomet provides the special operations for characterization of SSM structure as well as the standard operations applied in commonly used image analyzers. The following special operations are presented for discussion.

Evaluation of the distribution of porosity, eutectic content (continuous and occluded) and silicon content across the specimen. The silicon content is calculated from the eutectic content by the rule of the segments:

$$Si\ wt.\%=b+Q_{eu}*(d-b), \quad (2)$$

where b is the silicon solubility in the alpha solid-solution at the eutectic temperature; d is the silicon content at the eutectic point and Q_{eu} is eutectic fraction determined by image analysis.

Evaluation of special shape factor of the grains. A special grain shape factor is calculated in studies of anodized specimens in polarized light (Fig.6).

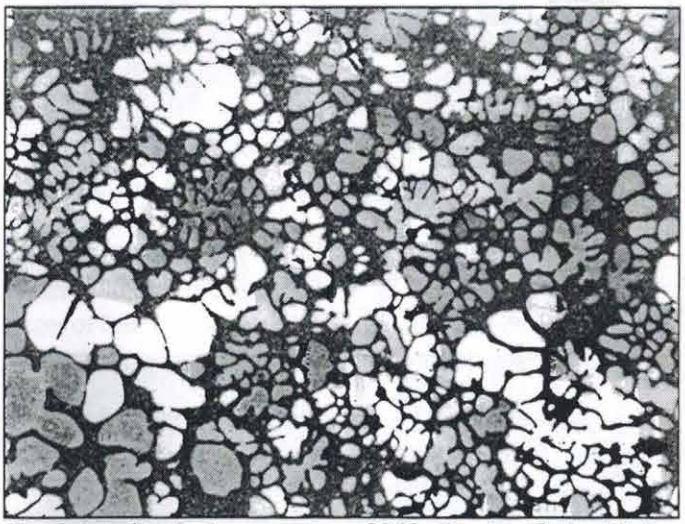

Fig.6. Anodized microstructure of 357 alloy in polarized light, 50X

The identification and integration of the dendrite's fragments, revealed in the planar image, into one structural isolated object is possible as a result of this measurement. A dimensionless grains shape factor F_g represents the area of a specific interface surface relative to that of one structurally isolated grain [10]:

$$Fg=\frac{1}{6\pi}\cdot\frac{S_V^2}{f_z\cdot N_A}, \quad (3)$$

where N_A is the number of structurally isolated grains per unit area; f_z is the volume fraction of alpha solid-solution grains; and, S_V is the area of the alpha solid-solution - eutectic interface per unit volume.

Referring to [2], the magnitude of S_V is proportional to the length of boundary lines of alpha solid-solution L_{zl} on the microsection with the area A:

$$S_V=\frac{4}{\pi}\cdot\frac{L_{zl}}{A} \quad (4)$$

So, the shape factor of the thixotropic grains can be evaluated taking into account the structural connections between its fragments. In this approach, the total specific length of interface boundaries is a function of the number of identified structurally isolated objects and not to the overall number of grains revealed in a given field of view. The grains are grouped on the principle of their identical crystallographic orientation. This fact is fixed by common color of these grains. Formal parameters by which the objects are combined with each other are the grayscale level of these objects and the distance between them (Fig.7).

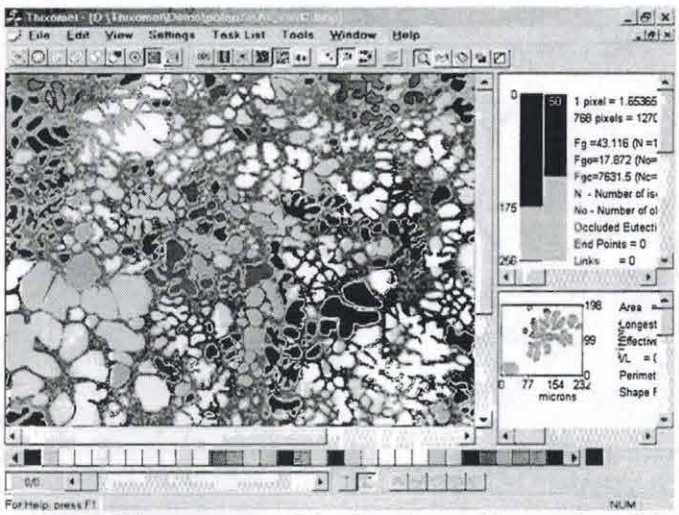

Fig.7. Thixomet screen. Identification and integration of the dendrite's fragments into structural isolated object

Three-dimensional reconstruction of the structure. 3D-structural reconstruction by sequential polishing of the semi-solid material has been carried out to check the adequacy of the grain morphology estimation using the shape factor F_g from the Eq.3. The images of the structure (with previously placed microhardness indentations for registration) were saved as graphic files. These files were used for precise positioning of the planar images in 3D space. The spacing between adjacent images was calculated by the change in the indentation size with polishing cycles.

To reconstruct the real picture of the 3D space connections of the grains, the processing of binary images was carried out as follows:

- an Euclidean Distance Map (EDM) was constructed of both the grains and the background (Fig.8). From the EDM, topological characteristics of the objects (end points, links, loops and branches) and a skeleton were determined to obtain the morphology information. The EDM of the background containing the information on object clustering could be used to determine the criteria of uniform distribution of the objects across the microsection [3];
- separating of touching grains was carried out (Fig 9);
- a 2D skeleton of the objects was produced (Fig 9).

The results of these studies were sufficient for the development of a unique 2D presentation procedure of the 3D reconstruction results (Figs 10-11).

Evolution is the procedure that works with the stored images of sequentially examined sections. These images are loaded into the PC memory. Using the scroll bar, the user outputs the sequential images to the Thixomet main window. As the adjacent images are replaced, the grain configurations

and their colors are changed (colors are replaced by textures in the Fig. 10). The user observes these changes according to the true connection of the grains in 3D space: the grains that are connected with each other in 3D space are the same in color and the user watches the color expansion.

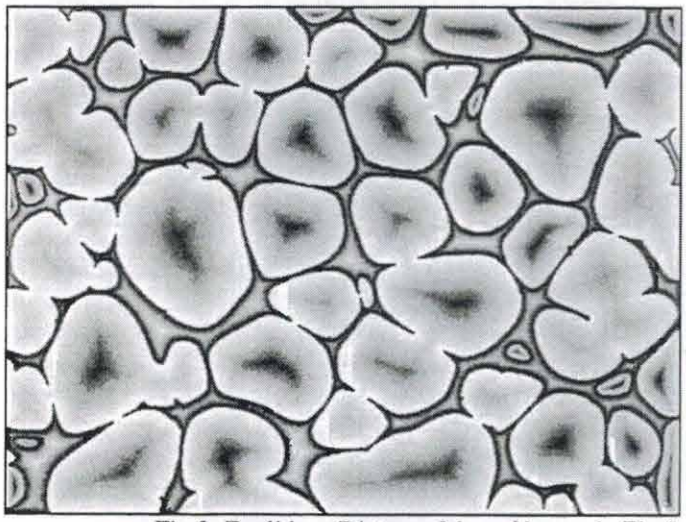

Fig.8. Euclidean Distance Map of image in Fig.5

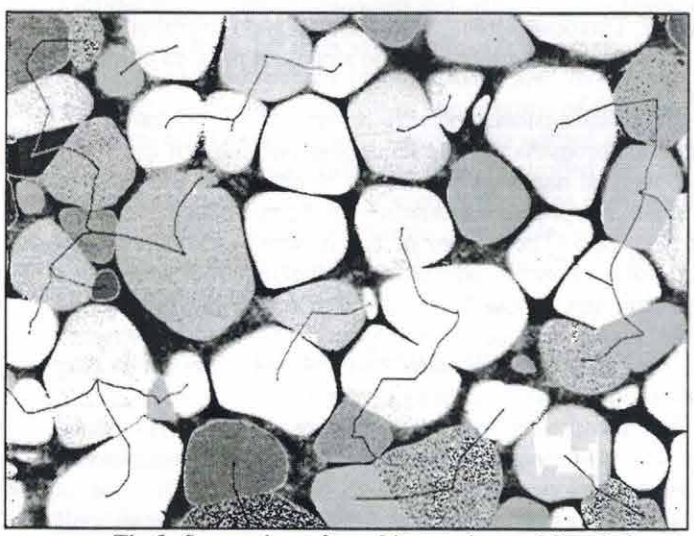

Fig.9. Separating of touching grains and 2D skeleton

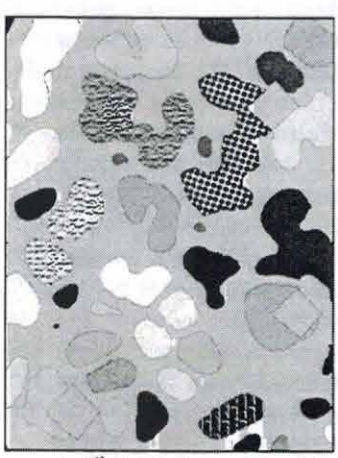

a) 1st field, 0 μm, $F_g = 4.2$

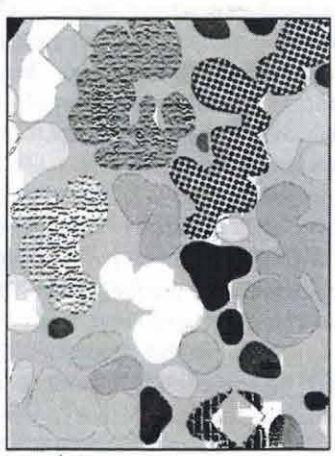

b) 5th field, 8 μm, $F_g = 4.4$

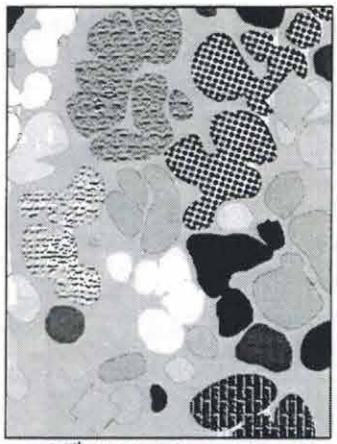

c) 10th field, 16 μm, $F_g = 5.7$

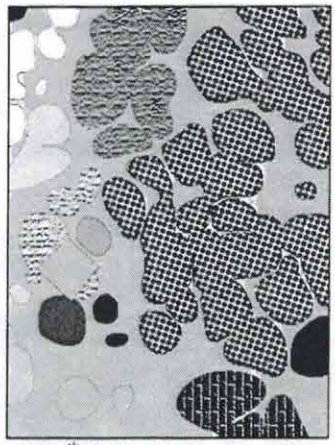

d) 15th field, 24 μm, $F_g = 5.3$

Fig.10. Steps of evolution procedure

Thus, as the number of analyzed images changes, the connectivity extent of the structure and corresponding shape factor value of the grains also change (Fig.10).

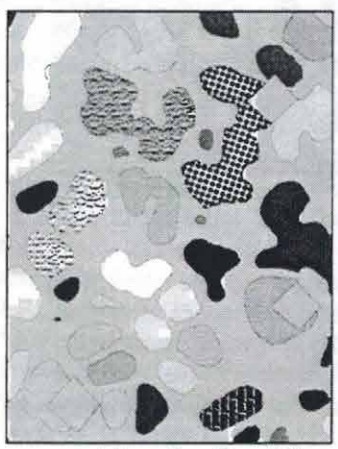

a) 1 section $F_g = 4.2$

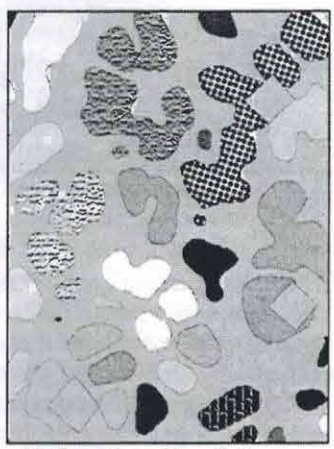

b) 5 sections $F_g = 5.4$

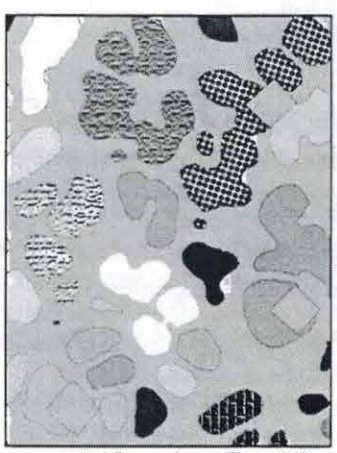

c) 10 sections $F_g = 5.9$

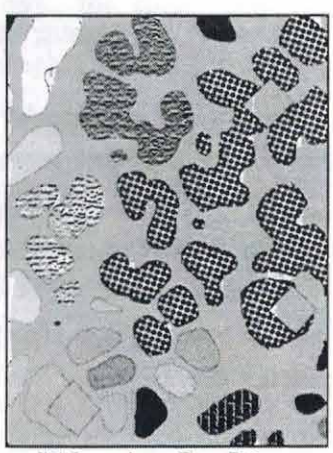

d)15 sections $F_g = 7.1$

Fig.11. Steps of identification procedure

Identification is a procedure that also works with the stored images of sequentially examined metallographic sections. However, the user observes only the first image of the first field of view, that is, the grain configuration is fixed

during the analysis. Using the scroll bar, the stored loaded images of the sequentially examined sections are analyzed step-by-step within the PC memory. As a result of this analysis, the user observes the expansion of colors (colors are replaced by textures in the Fig. 11) in accordance with the real connection of the grains in 3D space. Thus, as the number of analyzed sections changes, the connectivity extent of the structure and corresponding shape factor value of the grains also change (Fig. 11).

The analysis of the real connectivity of the grains in 3D space by the Evolution and Identification procedures revealed that the method of grain integration, according to the criterion of identical crystallographic orientation, is not sufficient. This is explained by the dual nature of thixotropic grain connectivity, namely, structural and technological. The structural nature relates to the identical crystallographic orientation of the grains, inherited from the dendrites. The technological nature of the grain connections relates to the collisions and welding, Ostwald ripening and coalescence of separate thixotropic grains into a common skeleton at all stages of SSF technology. The technological nature of the grain connections cannot be identified only by the crystallographic orientation criterion.

Therefore, the studies of anodized specimens in polarized light can be carried out only for the estimation of the structural connection of the grains and for the as-cast state only. These studies cannot be applied to the investigation of the samples in the as-reheated and as-formed conditions. The connection of the grains in these cases relates mainly to their technological nature. Therefore, the grain shape factors and the extent of their connectivity can be adequately estimated only from the results of the 3D reconstruction of the structure.

3D skeleton. The next step towards image processing in 3D is the determination of the 3D skeleton that simplifies the structure. The skeleton in 3D is formed by connecting the ultimate eroded points of the 2D sections (Fig.12).

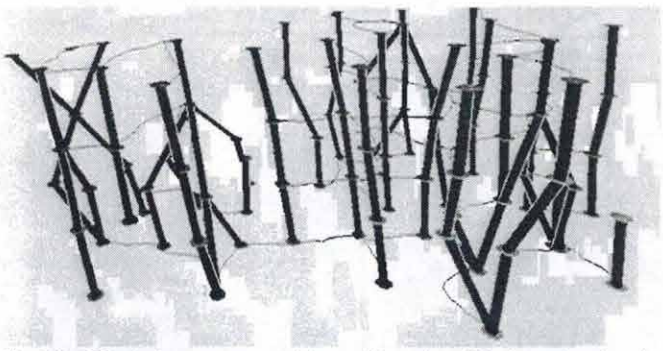

Fig.12. 3D skeleton zoomed by z-direction (skeletonization in 3D of the biggest conglomerate of grains in Figs.10-11)

It correctly depicts the topological properties of the structure closely related to the shape parameters. The connectivity of a skeletal structure is a topological property that is directly related to rheological properties. Since our first studies of the 3D skeleton were carried out, a multiple connected skeleton was found in the structure of semi-solid materials. Multiple connectivity denotes that some nodes may be connected to another by more that one path through the skeleton.

For the quantitative estimation of connectivity of multiply-connected structures, the first Betti number of the network (in our case the network is the skeleton), p_1, is best to use [11]. This number is defined as the number of branches in excess of the number required to form a tree (p_1=0) between the nodes in the skeleton [11]:

$$p_1 = b - n + p_0 \tag{5}$$

where b is the number of branches; n is the number of nodes and p_0 is the number of disconnected skeletons (first Betti number).

Thus, the connectivity of the structure is the number of branches that could be removed from the skeleton without creating additional separate parts.

3D reconstruction of the grains surface. Mert Flemings and his colleagues have already described the single agglomerate of alpha-grains present in thixotropic Al - 6.5 wt % Si alloy specimens, which were obtained by mechanical stirring under laboratory conditions [12]. To reconstruct the 3D structure of the agglomerate, a set of photographs was used in this study. In another work [13], the detailed computerized 3D reconstruction of the structure by microstructural tomography and analysis of the skeletal network was presented. The authors investigated the Ostwald ripening mechanism of Sn particles in a Pb-Sn eutectic. But, such 3D reconstructions for the commercial SSM have not been carried out until now.

The final stage of image processing in 3D is 3D reconstruction of the grain surfaces with the possibility of the analysis and presentation of the real surfaces of the grains (Fig.13).

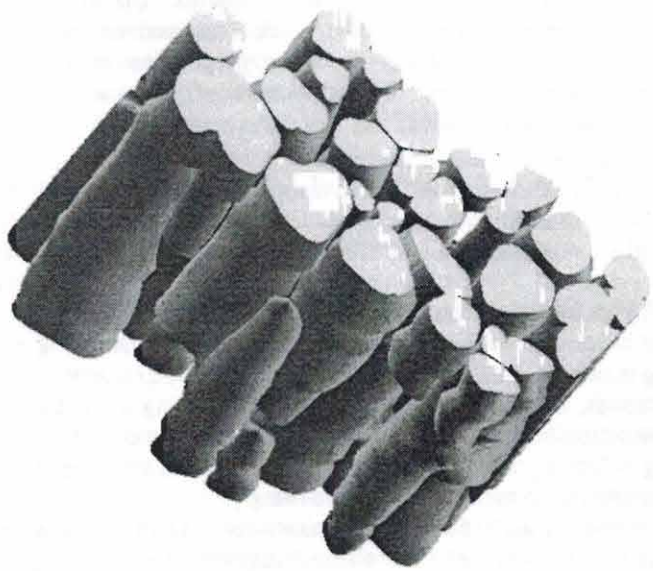

Fig.13. Thixomet 3D reconstruction of the real surfaces of the grains (zoomed by z-direction)

The unique algorithms in Thixomet 3D software permit execution of much faster three dimensional operations than similar procedures implemented in the most popular libraries for 3D graphics.

The capabilities of the Thixomet 3D software can be summarized as follows:

- 3D structural reconstructions using sequential planar examination;
- all operations with 3D image viewing (rotation, shifting, enlargement);
- three-dimensional measurements of the objects;
- computation and visualization of any profile of the object at the intersection with any sectioning plane;
- computation and visualization of intersection boundaries of several objects;
- image import-export in STL format.

In practice, the Thixomet 3D program can be utilized for three-dimensional measurements, modeling and designing developments.

Investigation of SSM. Thixomet capabilities have been used for comparison investigations of commercial SSM.

Materials and method. The samples were obtained from three companies (suppliers of SSM). Let us represent them as suppliers number 1, 2 and 3 and their samples were coded as 1, 2 and 3, respectively. The 357 alloy samples for the studies measured 15 × 15 × 76 mm and were machined from the 76 mm diameter billet. All studies were carried out in the as-cast state at 200× magnification except for two samples from supplier 1 (sample codes 1-2 and 1-A), which were in the as-reheated state, and were examined at 100×. The reheating procedure was as follows: the samples were held for 8 min at 587°C and quenched in water.

Metallographic imaging used the reflected light provided by a MeF3A Reichert-Jung metallograph with field positioning based upon microhardness indents. Up to 50 sequential parallel planes-of-polish were examined on each specimen using conventional specimen preparation with a Buehler Automet device. The thickness of the material removed was 29-42 μm for the as-cast specimens and 70 - 123 μm for the as-reheated specimens.

Results and discussion. The investigations of the nature of the silicon distribution across the billet's section revealed the distinctive segregation in specimen 3 in comparison with specimens 1 and 2 (Fig.14).

The increased silicon content inside the near-surface layer of the billet can cause the eutectic to flow out of the slug during reheating. Besides, with increasing of silicon content in local zones, the temperature at which the melting of alpha solid-solution begins rises and the process of eutectic melting during reheating slows down. As a result, there are coarse silicon crystals in such zones of the casting.

Figures 15 and 16 show the microstructures of the first and last fields of view for all investigated samples. The determination grain connectivity, based upon a common color, was carried out by the procedures of Evolution and Identification. Grains are artificially textured in accordance with their real 3D connections in Fig.15 and Fig.16. The same texture of the grains denotes that they are integrated into one skeleton.

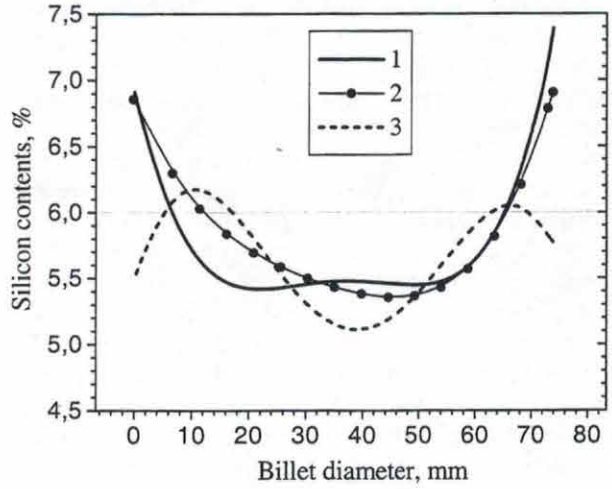

Fig.14.Silicon distribution across the billet's diameter

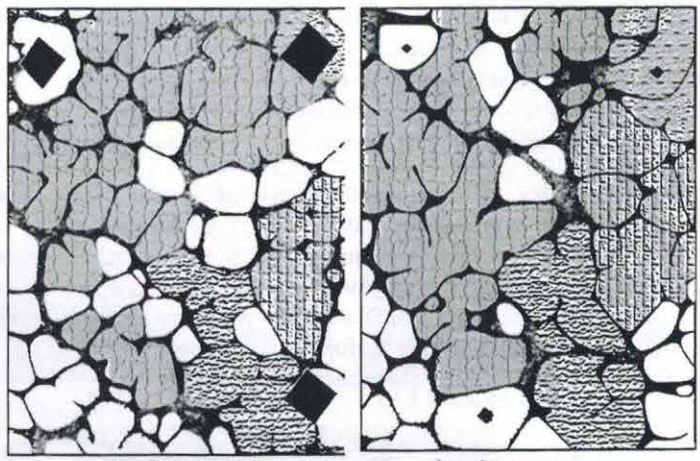

first image last image

a) sample 1, depth of analysis - 41 μm

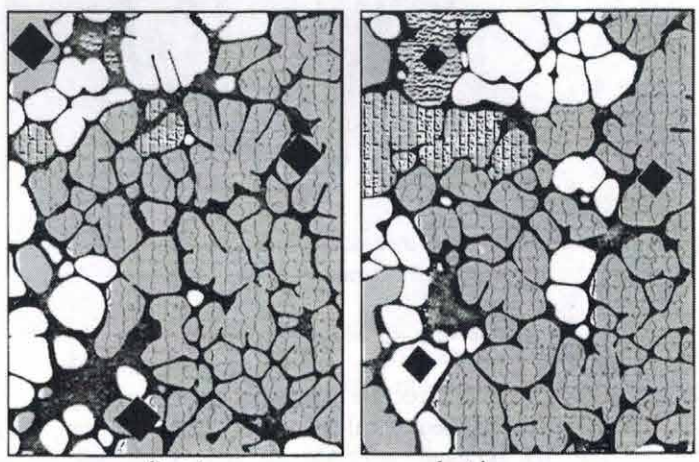

first image last image

b) sample 2, depth of analysis - 28 μm

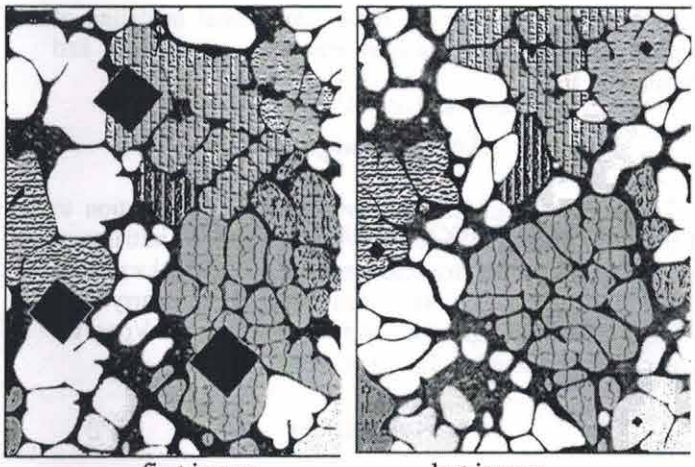

first image last image

c) sample 3, depth of analysis - 42 μm

Fig.15. Images of first and last fields of view of as cast samples, 200X.

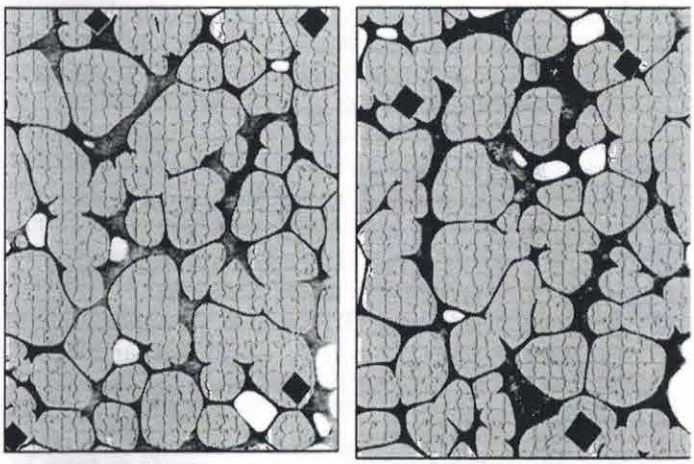

first image last image

a) sample 1-2, depth of analysis - 70 μm

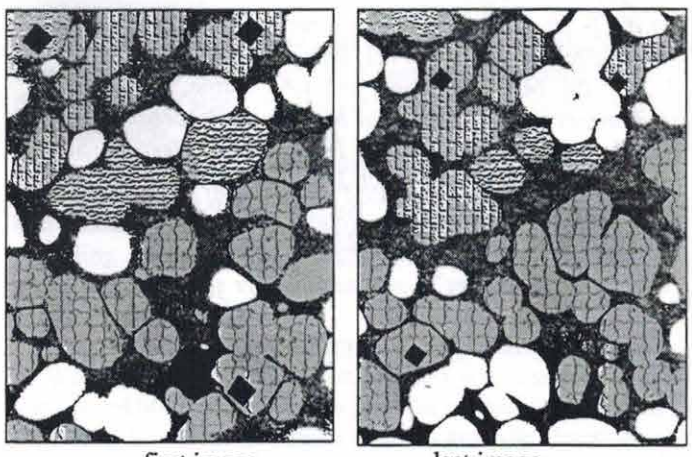

first image last image

b) sample 1-A, depth of analysis – 123 μm

Fig.16. Images of first and last fields of view of as reheated samples, 100X.

The data of 3D reconstruction of the samples are shown in Table 1.

Table 1. 3D reconstruction data of the investigated samples

Sample number		1	2	3	1-A	1-2
Depth of analysis, μm		41	29	42	123	70
Eutectic content, %		24	28	32	37	21
Sample state		as cast			as reheated	
1. Skeletons numbers	p_0	8	7	13	6	2
	$\cdot 10^3$ mm^{-3}	6.7	8.3	10.7	0.25	0.14
2. Structure connectivity	p_1	39	49	31	14	34
	$\cdot 10^4$ mm^{-3}	3.3	5.8	2.5	0.06	0.24
3. Connectivity for each of 6 bigger skeletons:	1	32	45	12	9	34
	2	5	2	6	4	0
	3	1	1	6	1	-
	4	1	1	3	0	-
	5	0	0	2	0	-
	6	0	0	2	0	-
5. Grains number integrated into each of 6 bigger skeletons, %	1	47	68	23	42	96
	2	13	5	18	18	1
	3	11	5	14	7	-
	4	8	3	11	6	-
	5	3	3	6	4	-
	6	2	2	3	3	-
6. Shape factor, F_g	by 1st field	10	21	16	10	24
	by last field	10	11	15	9	23

These results are sufficient to allow definite conclusions as to the structural quality of the investigated samples.

There is a minimum structural connectivity (p_1=31 or $2.5 \cdot 10^4$ 1/mm^3) in specimen 3. Thirteen fine skeletons ($10.7 \cdot 10^3$ 1/mm^3) were revealed inside this sample and all grains were rather uniformly integrated into six separate bigger skeletons. Skeleton connectivity was proportional to skeleton size: the greater the number of grains integrated into the skeleton, the higher the multiple connectivity.

Specimen 2 was the most multiply connected (p_1=49 or $5.8 \cdot 10^4$ 1/mm^3) as most of the grains (68%) were integrated into one multiply connected skeleton (p_1=45).

Specimen 1 was intermediate in structural quality between specimens 2 and 3. A large part of the excess connections (32 of 39) in this sample, along with specimen 2, was accounted for by one huge skeleton, which combined 47% of the total number of grains. The rest of the grains were sufficiently uniformly distributed among five small skeletons, that had few excess connections.

Thus, if a structure with minimum skeletonization and minimum multiple connectivity is necessary to ensure rheological properties for SSM, the as-cast samples would be

arranged in following decreasing order - 3, 1, 2 - as to their suitability for SSF technology.

There are evident changes in the structure of the specimens after reheating. With regards to microscope magnification and polishing depth, the investigated volume of the specimens in as-reheated state was 12-28 times larger than the volume of the specimens in as-cast state. Specific connectivity of the structure in the as-reheated state was many factors of ten smaller than in as-cast state because of structural coarsening and Ostwald ripening processes. It should be noted that eutectic quantity has a determining influence upon the skeletonization process and the formation of excess connections during reheating. The decrease in the eutectic content from 37% in specimen 1-A to 21% in the specimen 1-2 causes the structure of specimen 1-2 to be entirely skeletonized: 96% of all grains are combined within a single multiply connected skeleton (p_1=34 or $0.24 \cdot 10^4$,1/mm^3).

It is necessary to note that the values for the shape factor, F_g, calculated for the first and the last fields of view for the same sample, distinctly differ for the sample 2 despite the adequate estimation of N_A (Eq.3) by the methods of 3D reconstruction. Such F_g does not represent the special features of the structure. In this case, we have estimated an area of the alpha solid-solution - eutectic interface per unit volume (S_V) from Eq.4. More objective information on the shape factor could be obtained from the results of total 3D reconstruction by the direct 3D measurements of S_V .

So, the study revealed that the SSM structure has been totally skeletonized. Therefore, a multiply connected skeleton of the structure is a key attribute of SSF technology, which greatly influences the rheological properties of SSM. Such a skeleton is an inherent characteristic for all SSM suppliers. Many of SSF technology problems cannot be solved without an understanding of the nature of skeleton structural formation and its evolution at all stages of SSM production.

Thixomet software performs a total quantitative description of 2D and 3D SSM structures, including 3D parameters of the structural skeleton and the real morphology of the alpha grains. We developed a special tool, which offers direct visualization and measurement of complex structures and 3D relationships.

The next step in the growth of the Thixomet approach will be to further develop criteria and standards for quality estimation of SSM 3D structures for industrial application. Such an approach will permit us to carry out analysis of SSM quality at all production stages. The results of this analysis will be useful for SSF technology improvement.

Summary and Conclusion

The Thixomet family of products for characterization of the structure of materials have been developed. Capabilities of Thixomet, Thixomet SAQE and Thixomet 3D have been demonstrated with examples of quality estimation of nickel-based superalloys and aluminum-based semi-solid materials.

Developed 3D procedures and algorithms can be effectively applied, not only for 3D materials structural characterization, but also for three-dimensional modeling of physical processes such as heat and mass transferring and deformation.

Acknowledgments

The authors gratefully acknowledge the contribution to this research of Daniel Adenis, who was also an initiator of work in SSM structure characterization. Special thanks are due to Svetlana Pavlova, who has helped to carry out metallographic investigations and to George Vander Voort for his moral support and fruitful discussions.

References

1. E.E. Underwood, *Quantitative Stereology*, p. 274, Reading, MA: Adison-Wesley Publishing Company (1970)
2. S.A. Saltykov, *Stereometric metallography*, p. 446, Metallurgizdat, Moscow (1958)
3. John C. Russ, *The Image Processing Handbook*, p. 674, CRC Press, USA (1995)
4. John C. Russ, *Practical Stereology*, p. 185, Plenum Press, New York and London (1991)
5. A. A. Kazakov and N.H. Luong, Official registration certificate of the software for PC № 980415
6. A. A. Kazakov and N.H. Luong, Official registration certificate of the software for PC № 990561
7. A. A. Kazakov and N.H. Luong, Official registration certificate of the software for PC № 990562
8. A. Kazakov, N. Luong, E. Kazakova, *Proceedings of International Conference on Quantitative Description of Materials Microstructure*, Warsaw, 337-42 (1997).
9. S.P. Midson, K. Brissing, *Modern casting*, 2, 41-3 (1997)
10. W.R. Loue and M. Suery, *Material Science and Eng.*, A203, 1-13 (1995)
11. R.T. De Hoff, E.H. Aigeltinger and K.R. Craig, *J. Of Microscopy*, Vol.95, Pt1, Feb., 69-91 (1972)
12. Y. Ito, M.C. Flemings, and J.A. Cornie, *Nature and properties of Semi-Solid Materials/ Proceeding of a symposium, held during 1992 Annual Meeting*, San Diego, California, March 1-5, 3-17 (1992)
13. T.L. Wolfsdorf, W.H. Bender and P.W. Voorhees, *Acta mater.*, Vol.45, 6, 2279-95 (1997)